

HOTCAKE: Higher Order Tucker Articulated Kernels for Deeper CNN Compression

Rui Lin¹, Ching-Yun Ko², Zhuolun He³, Cong Chen⁴, Yuan Cheng⁵, Hao Yu⁶, Graziano Chesi⁷, Ngai Wong⁸,

¹rlin@eee.hku.hk, ²cyko@mit.edu, ³zleonhe@gmail.com, ⁴chencong@eee.hku.hk,
⁵cyuan328@sjtu.edu.cn, ⁶yuh3@sustc.edu.cn ⁷chesi@eee.hku.hk, ⁸nwong@eee.hku.hk,

Abstract—The emerging edge computing has promoted immense interests in compacting a neural network without sacrificing much accuracy. In this regard, low-rank tensor decomposition constitutes a powerful tool to compress convolutional neural networks (CNNs) by decomposing the 4-way kernel tensor into multi-stage smaller ones. Building on top of Tucker-2 decomposition, we propose a generalized Higher Order Tucker Articulated Kernels (HOTCAKE) scheme comprising four steps: input channel decomposition, guided Tucker rank selection, higher order Tucker decomposition and fine-tuning. By subjecting each CONV layer to HOTCAKE, a highly compressed CNN model with graceful accuracy trade-off is obtained. Experiments show HOTCAKE can compress even pre-compressed models and produce state-of-the-art lightweight networks.

Index Terms—Convolutional neural network, Higher order Tucker decomposition

I. INTRODUCTION

Deep learning and deep neural networks (DNNs) have witnessed breakthroughs in various disciplines, e.g., [1], [2]. However, the progressively advanced tasks, as well as the ever-larger datasets, continuously foster sophisticated yet complicated DNN architectures. Despite the sentiment that the redundancy of parameters contributes to faster convergence [3], over-parameterization unarguably impedes the deployment of modern DNNs on edge devices constrained with limited resources. This dilemma intrinsically highlights the demand of compact neural networks. Mainstream DNN compression techniques roughly comprises three categories, namely, pruning, quantization and low-rank decomposition, as depicted below: *Pruning*—It trims a dense network into a sparser one, either by cropping the small-weight connections between neural nodes (a.k.a. fine-grained) [4], or by removing entire filters and/or even layers (a.k.a. coarse-grained) via a learning approach [5], [6].

Quantization— It limits network weights and activations to be in low bit-widths (e.g., zero or powers of two [7]) such that expensive multiplications are replaced by cheap shift operations. As extreme cases, binary networks such as BNN [8] and XNOR-Net [9] use only 1-bit representation that largely reduces computation, power consumption and memory footprint, but at the cost of sometimes drastic accuracy drop.

Low-rank decomposition— Initially, low-rank singular value decomposition (SVD) was performed on fully connected (FC) layers [10]. It was later recognized that filters of a CONV layer can be aggregated as a 4-way kernel (filter) tensor

(height \times width \times #inputs \times #outputs) and decomposed into low-rank factors for compression. For example, Ref. [11] uses canonical polyadic (CP) decomposition to turn a CONV layer into a sequence of four convolutional layers with smaller kernels. However, this approach only compresses one or several layers instead of the whole network. Its manual rank selection also makes the procedure time-consuming and ad-hoc. Ref. [12] overcomes this by utilizing Tucker-2 decomposition to factorize a CONV layer into three successive stages of smaller kernels, whose corresponding Tucker ranks are searched via Variational Bayesian Matrix Factorization (VBMF). Ref. [13] surveys various tensor decompositions and their use in compressing CONV layers empirically. However, all these works invariably adopt a 4-way view of the convolutional kernel tensor.

This work is along the line of tensor decomposition, and recognizes the unexploited rooms for deeper compression by going beyond 4-way. Specifically, we show, for the first time, that it is possible to further tensorize the #inputs axis into smaller modes, and as a result achieve higher compression with a tolerable accuracy drop. Our key contributions are:

- We lift the 4-way bar of viewing a CNN kernel tensor and relax the Tucker-2 decomposition [12] to arbitrary orders. We subsequently propose **H**igher **O**rders **T**uCKER **A**rticulated **K**ERnels (HOTCAKE) for granular CONV layer decomposition into smaller kernels and potentially higher compression.
- Although VBMF provides a principled way of Tucker rank selection, it does not guarantee a global or locally optimal combination of ranks. To this end, we adapt the rank search in a neighborhood centered around VBMF-initialized ranks. Such finite search space largely alleviates the computation of traditional grid search and locates a locally optimal combination of Tucker ranks that work extremely well in practice.
- HOTCAKE is tangential to other compression techniques and can be applied together with pruning and/or quantized training etc. Being a generic technique, it can be applied to all CNN layers, which is crucial since nowadays fully convolutional networks (FCNs) [14] are widely used in autonomous driving and robot navigation etc.

Experimental results on some state-of-the-art networks then demonstrate that HOTCAKE produces models that strike

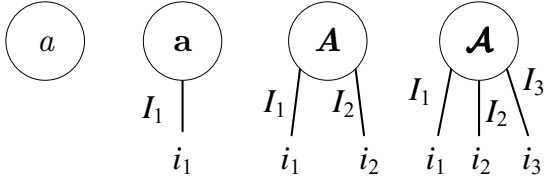


Fig. 1. Graphical representation of a scalar a , vector \mathbf{a} , matrix \mathbf{A} , and third-order tensor \mathcal{A} .

an elegant balance between compression and accuracy, even when compressing a pre-compressed neural network. In the following, Section II introduces some tensor basics. Section III introduces HOTCAKE. Section IV presents the experimental results and Section V concludes the paper.

II. TENSOR BASICS

Tensors are multi-way arrays that generalize vectors (viz. one-way tensors) and matrices (viz. two-way tensors) to their higher order counterparts [15]. Henceforth, scalars are denoted by Roman letters a, b, \dots ; vectors by boldface letters $\mathbf{a}, \mathbf{b}, \dots$; matrices by boldface capital letters $\mathbf{A}, \mathbf{B}, \dots$ and tensors by boldface capital calligraphic letters $\mathcal{A}, \mathcal{B}, \dots$. Figure 1 shows the so-called *tensor network diagram* for these data structures where an open edge or “leg” stands for an index axis. For a d -way tensor $\mathcal{A} \in \mathbb{R}^{I_1 \times I_2 \times I_3 \times \dots \times I_d}$, $\mathcal{A}(i_1, i_2, \dots, i_d)$ denotes an entry, i_k ($1 \leq i_k \leq I_k$) is the index on the k mode with a dimension I_k . A fiber of tensor \mathcal{A} is obtained by fixing all indices but one. For example, we get a k -mode fiber $\mathcal{A}(i_1, \dots, i_{k-1}, :, i_{k+1}, \dots, i_d) \in \mathbb{R}^{I_k}$ by fixing all other mode indices and scanning through i_k . In other words, fibers are high-dimensional analogues of rows and columns in matrices. Employing *numpy*-like notation, “`reshape(\mathcal{A} , [m_1, m_2, \dots, m_p])`”, a d -way tensor $\mathcal{A} \in \mathbb{R}^{I_1 \times I_2 \times I_3 \times \dots \times I_d}$ is reshaped into another tensor with dimensions m_1, m_2, \dots, m_p that satisfies $\prod_{k=1}^p m_k = \prod_{k=1}^d I_k$. Tensor *permutation* rearranges the mode ordering of tensor \mathcal{A} , while keeping the total number of tensor entries unchanged. Tensor-matrix multiplication or *mode product* is a generalization of matrix-matrix product to that between a matrix along one mode of a tensor:

Definition 1: (k -mode product) The k -mode product of tensor $\mathcal{G} \in \mathbb{R}^{R_1 \times \dots \times R_d}$ with a matrix $\mathbf{U} \in \mathbb{R}^{J \times R_k}$ is denoted $\mathcal{A} = \mathcal{G} \times_k \mathbf{U}$ and defined by

$$\mathcal{A}(r_1, \dots, r_{k-1}, j, r_{k+1}, \dots, r_d) = \sum_{r_k=1}^{R_k} \mathbf{U}(j, r_k) \mathcal{G}(r_1, \dots, r_{k-1}, r_k, r_{k+1}, \dots, r_d)$$

where $\mathcal{A} \in \mathbb{R}^{R_1 \times \dots \times R_{k-1} \times J \times R_{k+1} \times \dots \times R_d}$.

With these definitions, the full multilinear product [16] of a d -way tensor and d matrices quickly follows:

Definition 2: (Full multilinear product) The full multilinear product of a tensor $\mathcal{G} \in \mathbb{R}^{R_1 \times \dots \times R_d}$ with matrices $\mathbf{U}^{(1)}, \mathbf{U}^{(2)}, \dots, \mathbf{U}^{(d)}$, where $\mathbf{U}^{(k)} \in \mathbb{R}^{I_k \times R_k}$, is defined by $\mathcal{A} = \mathcal{G} \times_1 \mathbf{U}^{(1)} \times_2 \mathbf{U}^{(2)} \dots \times_d \mathbf{U}^{(d)}$, where $\mathcal{A} \in \mathbb{R}^{I_1 \times \dots \times I_d}$.

Now the Tucker decomposition follows:

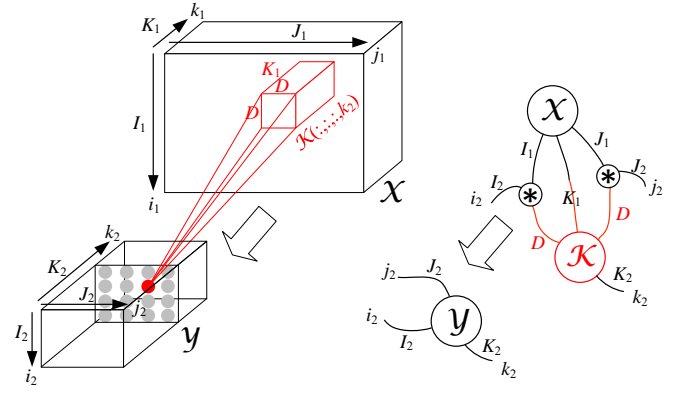


Fig. 2. Convolution with the input tensors and the kernels.

Definition 3: (Tucker decomposition) Tucker decomposition represents a d -way tensor $\mathcal{A} \in \mathbb{R}^{I_1 \times \dots \times I_d}$ as the full multilinear product of a core tensor $\mathcal{G} \in \mathbb{R}^{R_1 \times R_2 \times \dots \times R_d}$ and a set of factor matrices $\mathbf{U} \in \mathbb{R}^{I_k \times R_k}$, for $k = 1, 2, \dots, d$. Writing out $\mathbf{U}^{(k)} = [\mathbf{u}_1^{(k)}, \mathbf{u}_2^{(k)}, \dots, \mathbf{u}_{R_k}^{(k)}]$ for $k = 1, 2, \dots, d$,

$$\begin{aligned} \mathcal{A} &= \sum_{r_1=1}^{R_1} \dots \sum_{r_d=1}^{R_d} \mathcal{G}(r_1, \dots, r_d) (\mathbf{u}_{r_1}^{(1)} \circ \dots \circ \mathbf{u}_{r_d}^{(d)}) \\ &= \mathcal{G} \times_1 \mathbf{U}^{(1)} \times_2 \mathbf{U}^{(2)} \dots \times_d \mathbf{U}^{(d)} \end{aligned}$$

where r_1, r_2, \dots, r_d are auxiliary indices that are summed over, and \circ denotes the outer product.

The dimensions (R_1, R_2, \dots, R_d) are called the *Tucker ranks*. We call $\text{rank}(\mathcal{A}_{(k)})$ the multilinear rank, and R_k is in general no bigger than it. Analogous to SVD truncation, the R_k 's can be truncated yielding a Tucker approximation to the original (full) tensor \mathcal{A} .

III. HOTCAKE

In each CNN layer, the convolutional kernels form a 4-way tensor $\mathcal{K} \in \mathbb{R}^{D \times D \times K_1 \times K_2}$, where $D \times D$ are the spatial dimensions, whereas K_1 and K_2 are the numbers of input and output channels, respectively. Figure 2 illustrates through tensor network diagram how convolution is done via a particular kernel (filter) producing the k_2 th slice in the output tensor (a.k.a. feature map). Specifically, a CNN filter $\mathcal{K}(:, :, :, k_2) \in \mathbb{R}^{D \times D \times K_1}$ strides across the input tensor $\mathcal{X} \in \mathbb{R}^{I_1 \times J_1 \times K_1}$ in the spatial dimensions to produce the k_2 th slice in the output tensor $\mathcal{Y} \in \mathbb{R}^{I_2 \times J_2 \times K_2}$. In the tensor network diagram, we adopt the convolution symbol \circledast from [13] that abstracts the convolution along the input spatial dimensions to produce the corresponding output spatial dimensions, with stride and zero padding implicitly considered. Such notation hides the unnecessary details and captures the CNN flow clearly, thereby further justifying the benefits of tensor network diagrams.

The basis of HOTCAKE arises from the work in [12] that performs Tucker-2 decomposition on the mode-3 (#inputs) and mode-4 (#outputs) of the kernel tensor \mathcal{K} so as to decompose a convolutional layer into three smaller consecutive ones.

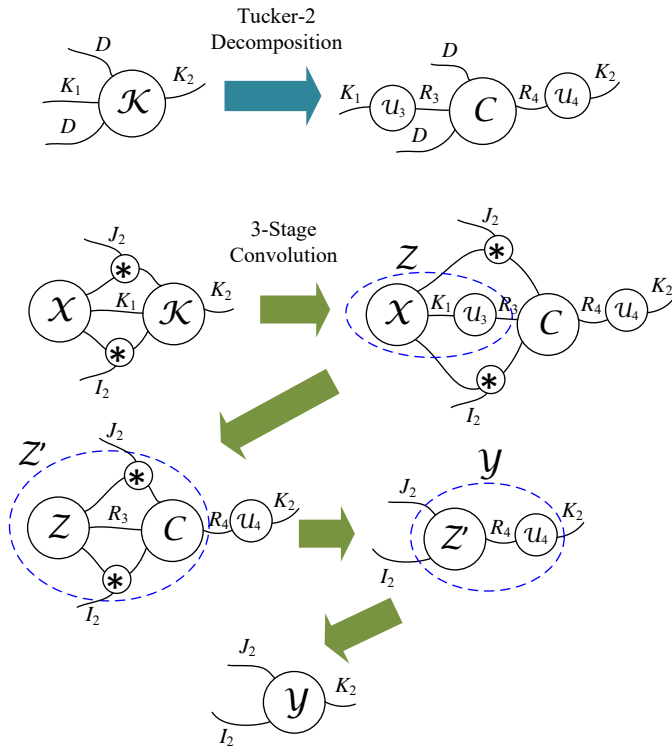


Fig. 3. (Upper) Tucker-2 decomposition of kernel tensor and (Lower) the three successive, smaller size convolutions marked by blue dashed circles. Some obvious dimensions are omitted in the figure for brevity.

Referring to the upper part of Figure 3, (R_3, R_4) are Tucker ranks of mode-3 and mode-4, respectively, and the kernel filters of the three smaller convolution layers are in order $\mathbf{U}_3 \in \mathbb{R}^{1 \times 1 \times K_1 \times R_3}$, $\mathbf{C} \in \mathbb{R}^{D \times D \times R_3 \times R_4}$ and $\mathbf{U}_4 \in \mathbb{R}^{1 \times 1 \times R_4 \times K_2}$. The dashed circles in the lower part of Figure 3 depicts the 3-stage linear convolution that replaces the original convolution before the nonlinear activation. Contrasting with the right of Figure 2 where there are two legs with the convolution operator \circledast in which it is assumed $D > 1$ (say, 3 or 5), such legs are not needed for $D = 1$ as in the first and third stages since the input and output feature maps share the same spatial “legs” due to the 1×1 nature. Consequently, instead of the one-step $\mathbf{Y} = \mathbf{X} \circledast \mathbf{K}$, it becomes $\mathbf{Z} = \mathbf{X} \circledast \mathbf{U}_3$, $\mathbf{Z}' = \mathbf{Z} \circledast \mathbf{C}$ and $\mathbf{Y} = \mathbf{Z}' \circledast \mathbf{U}_4$. And the number of kernel parameters goes from $D^2 K_1 K_2$ to $K_1 R_3 + D^2 R_3 R_4 + K_2 R_4$ with the latter being much smaller when R_3 and R_4 are small.

In short, HOTCAKE innovates by adopting an arbitrary-order perspective of the kernel tensor and allows higher order Tucker decomposition that results in even more granular linear convolutions through a series of small-size articulated kernels (and thereby its name). Moreover, other engineering improvements are incorporated to streamline HOTCAKE into a four-stage pipeline: (1) input channel decomposition; (2) Tucker rank selection; (3) higher order Tucker decomposition; (4) fine-tuning. Their details are described below.

A. Input channel decomposition

Example 1: Suppose a convolution layer of kernel tensor $\mathbf{K} \in \mathbb{R}^{3 \times 3 \times 128 \times 256}$. In this case, the number of input channels is $K_1 = 128$, which can be decomposed into several branches of dimensions K_{1i} 's such that $K_1 = \prod_i K_{1i}$, such as $K_{12} = 16$ and $K_{11} = 8$. These K_{1i} 's can be determined according to the estimated number of clusters of filters. Empirically, it is found that it works best when $K_{1j} \geq K_{1i}, \forall j \geq i$.

After decomposing the input channels into l branches, the 4-way kernel tensor $\mathbf{K} \in \mathbb{R}^{D \times D \times K_1 \times K_2}$ is reshaped into a $(3 + l)$ -way tensor $\mathbf{K}_{new} \in \mathbb{R}^{D \times D \times K_{11} \times \dots \times K_{1l} \times K_2}$. The reason that we do not factorize the #outputs axis is that the CONV layers are always followed by batch normalization and/or pooling. Such operations are generally done on a 3-way output tensor, and if we tensorize the #outputs axis into multi-way, we will need to reshape them back into one mode which increases the computation complexity. Also, Tucker decomposition is not carried out on the spatial dimensions $D \times D$ as they are inherently small, e.g., $D = 1, 3, 5$.

B. Tucker rank selection

Following from above, the rank- $(R_{3i}, \dots, R_{3l}, R_4)$ determines the trade-off between the compression and accuracy loss. A manual search of the ranks is time-consuming and does not guarantee appropriate ranks, whereas exhaustive grid-search guarantees the best combo but is prohibitive due to exponential combinations. To estimate the proper ranks, Ref. [12] employs the analytic Variational Bayesian Matrix Factorization (VBMF) that is able to find the variance noise and ranks, and thus offers a good yet sub-optimal set of Tucker ranks. To this end, HOTCAKE uses the VBMF-initialized ranks to center the search space and evaluates the rank combos in a finite neighborhood.

Example 2: Given a kernel tensor $\mathbf{K} \in \mathbb{R}^{3 \times 3 \times 128 \times 256}$, suppose the input channel decomposition makes it a $\mathbf{K}_{new} \in \mathbb{R}^{3 \times 3 \times 8 \times 16 \times 256}$ by decomposing its #inputs axis into 2 branches. Assuming selected VBMF ranks of \mathbf{K}_{new} being $(R_{31}, R_{32}, R_4) = (5, 7, 107)$ and a search diameter of 3, the rank search space in our algorithm is then $\{(R_{31}, R_{32}, R_4) | [4, 5, 6] \times [6, 7, 8] \times [106, 107, 108]\}$, containing 27 different combinations.

Compared with grid-search, our rank selection strategy searches a much smaller finite space and requires much lower computation. It also outweighs a pure VBMF solution, as searching within a region rather than sticking to a point gives a higher possibility to locate a better rank setting. Notably, we introduce randomized SVD (rSVD) [17] to the VBMF initialization in replace of conventional SVD to avoid the $\mathcal{O}(n^3)$ computational complexity, where n is the $\max(\#rows, \#columns)^1$.

¹Since the input channels are decomposed into several branches, the flattened matrix of tensor \mathbf{K}_{new} needed for VBMF usually has a very large #columns, leading to the failure of SVD. In contrast, rSVD overcomes this problem by randomly projecting the original large matrix onto a much smaller subspace, while producing practically same results in all our experiments.

C. Higher order Tucker compression

The truncated higher-order singular value decomposition (HOSVD) [18] and the higher-order orthogonal iteration algorithm (HOOI) [19] are two widely used algorithms for Tucker decomposition. Here, we employ HOSVD with rSVD in place of SVD as described before. Procedure 1 describes the modified HOSVD. We remark that the computation of

Procedure 1 Modified truncated higher-order singular value decomposition (HOSVD)

Require: Tensor $\mathcal{K}_{new} \in \mathbb{R}^{I_1 \times \dots \times I_d}$, ranks: R_1, \dots, R_d .

Ensure: Core tensor $\mathcal{G} \in \mathbb{R}^{R_1 \times \dots \times R_d}$, factor matrices $U^{(1)}, \dots, U^{(d)}$, where $U^{(k)} \in \mathbb{R}^{I_k \times R_k}$ for $k = 1, \dots, d$.

for $n = 1, 2, \dots, d$ **do**

$[\mathbf{L}, \Sigma, \mathbf{R}^T] \leftarrow$ rSVD decomposition of $\mathbf{K}_{new(n)}$

$U^{(n)} \leftarrow R_n$ leading left columns of \mathbf{L}

end for

$\mathcal{G} \leftarrow [[\mathcal{K}_{new}; U^{(1)T}, \dots, U^{(d)T}]]$

each factor matrix $U^{(n)}$ ($n = 1, \dots, d$) is independent, since the input matrix $\mathbf{K}_{new(n)}$ for rSVD is from the tensor \mathcal{K}_{new} independently. Thus, Tucker decomposition can be done on selected modes in parallel. For a given tensor \mathcal{K}_{new} , after Tucker decomposition, there are l 1×1 CONV layers and exactly one CONV layer with the same spatial filter size, stride and zero-padding size as the original CONV layer, but the dimensions of input channels and output channels are smaller. The following example shows how input data are convolved with those CONV layers.

Example 3: Given a kernel tensor $\mathcal{K} \in \mathbb{R}^{3 \times 3 \times 128 \times 256}$, suppose its input channels are decomposed into 2 modes. After Tucker decomposition, there are 4 tensors, denoted $\mathcal{U}_3 \in \mathbb{R}^{1 \times 1 \times 8 \times 5}$, $\mathcal{U}_4 \in \mathbb{R}^{1 \times 1 \times 16 \times 7}$, $\mathcal{C} \in \mathbb{R}^{3 \times 3 \times 35 \times 117}$ and $\mathcal{U}_5 \in \mathbb{R}^{1 \times 1 \times 117 \times 256}$. Note that the factor matrices $\mathcal{U}_3, \mathcal{U}_4, \mathcal{U}_5$ are tensorized with “singleton” axes and regarded as 4-way convolutional kernels as well. The rest of the flow then follows similarly to Figure 3, but now with two 1×1 CONV layers due to \mathcal{U}_3 and \mathcal{U}_4 , followed by the 3×3 CONV of \mathcal{C} and ended with another 1×1 CONV of \mathcal{U}_5 to produce \mathcal{Y} .

Next, we analyze the space and time complexities of a CONV layer in HOTCAKE. For storage, the parameter number is in $\mathcal{O}(D^2 R_{3i}^l + l R_{3i} K_{1i} + K_4 R_4)$, where R_{3i} and K_{1i} are the largest values in $R_{31}, R_{32}, \dots, R_{3l}$ and $K_{11}, K_{12}, \dots, K_{1l}$, respectively. We remark that K_{1i} is exponentially smaller than K_1 , and R_{3i} is further smaller than K_{1i} . Therefore, the overall parameter number in a decomposed layer is much smaller than the original $\mathcal{O}(D^2 K_1 K_2)$. For time complexity, assuming the output feature height and width are the same as those of the input feature after passing the CONV layer, the time complexity is $\mathcal{O}(M^2 (D^2 R_{3i}^l + l R_{3i} K_{1i} + K_4 R_4))$, where M is the output feature height or width value. Recognizing that the time complexity of the original CONV layer is $\mathcal{O}(M^2 D^2 K_1 K_2)$, a huge computational complexity reduction can be achieved.

D. Fine-tuning

After the above three stages, the accuracy of the Tucker decomposed model often drops significantly. However, the accuracy can be recovered to an acceptable level (in less than 20 epochs in all our trials) via retraining.

IV. EXPERIMENTAL RESULTS

We implement the proposed HOTCAKE processing on three popular architectures, namely, SimpNet [20], MTCNN [21] and AlexNet [1]. The first two are lightweight networks, while the last one is deeper and contains more redundant parameters. We use *CIFAR-10* [22] dataset as a benchmark for SimpNet and AlexNet. The datasets used for MTCNN are *WIDER FACE* and *CNN for Facial Point*. All neural networks are implemented with PyTorch, and experiments are run on an NVIDIA GeForce GTX1080 Ti Graphics Card with 11GB frame buffer. We compared HOTCAKE with Tucker-2 decomposition [12] but not with CP decomposition [11] because the latter can only be used to compress 1 or 2 CONV layers and not applicable to the whole network.

A. Experiments on SimpNet

We first tested with several lightweight CNNs, which aims to show that HOTCAKE can further remove the redundancy in some intentionally designed compact models. The first lightweight CNN we compressed is SimpNet [20]. This net is carefully crafted in a principled manner and has only 13 layers and 5.48M parameters, while still outperforming the conventional VGG and ResNet etc. in terms of classification accuracy. Due to its efficient and compact architecture, SimpNet can potentially achieve superior performance in many real-life scenarios, especially in resource-constrained mobile devices and embedded systems.

There are totally 13 CONV layers in the SimpNet and we do not compress the first layer since the input channel number is only 3. Table I shows the overall result when compressing the 2–13 CONV layers with Tucker-2 and HOTCAKE. We notice that the two methods achieve similar classification accuracy after fine-tuning, while HOTCAKE produces a more compact model. The detailed parameter number and compression ratio of each CONV layer are enumerated in Table II. We observe that HOTCAKE achieves a higher compression ratio than Tucker-2 almost in every CONV layer. Table II also provides hints as to which layer is the most compressible and one can better achieve a balance between the model size and the classification performance. For example, we can decide which layers should be compressed if a specific model size is given. Fig. 4 shows the classification accuracy of the compressed model obtained by employing HOTCAKE when increasing the number of compressed layers. The sequence we compress the CONV layer is determined by their compression ratios listed in Table II. The layers with higher compression ratio will be compressed at the beginning. Employing this strategy, we can achieve the highest classification accuracy when the overall model compression ratio is given.

TABLE I
AN OVERVIEW OF SIMPNET’S PERFORMANCE AND THE NUMBER OF PARAMETERS BEFORE AND AFTER COMPRESSION.

	Original	Tucker-2	HOTCAKE
Testing Accuracy	95.21%	90.84%	90.95%
Overall Parameters	5.48M	2.24M	1.75M
Compression Ratio		2.45×	3.13×

TABLE II
SIMPNET’S LAYER-WISE ANALYSIS. NUMBERS IN BRACKETS ARE COMPRESSION RATIOS COMPARED WITH THE ORIGINAL CONV LAYERS.

No. of compressed CONV layers	Original	Tucker-2	HOTCAKE
2	76K	30K (2.53×	24K (3.17×
3	147K	61K (2.41×	39K (3.77×
4	147K	61K (2.41×	43K (3.42×
5	221K	88K (2.72×	65K (3.40×
6	332K	136K (2.44×	103K (3.22×
7	332K	137K (2.42×	92K (3.61×
8	332K	137K (2.42×	104K (3.19×
9	332K	135K (2.46×	112K (2.96×
10	498K	206K (2.42×	162K (3.07×
11	746K	314K (2.37×	183K (4.08×
12	920K	371K (2.48×	257K (3.58×
13	1.12M	569K (1.97×	569K (1.97×

With the successful application on SimpNet, we argue that our proposed compression scheme can handle the already-tiny model better than Tucker-2. In the next experiment, we consider an even smaller CNN model and compress it using HOTCAKE.

B. Experiments on MTCNN

The second model we tested is MTCNN [21], which is designed for human face detection. Aiming for real-time performance, each built-in CNN in MTCNN is designed to be lightweight deliberately. Specifically, MTCNN contains three cascaded neural networks called Proposal Network (P-Net), Refinement Network (R-Net) and Output Network (O-Net). The size of P-Net and R-Net are too small such that we do not have much space to compress them. Therefore, we compress only the O-Net which contains 4 CONV layers with the kernel tensor of $\mathcal{K}^{(1)} \in \mathbb{R}^{3 \times 3 \times 3 \times 32}$, $\mathcal{K}^{(2)} \in \mathbb{R}^{3 \times 3 \times 32 \times 64}$, $\mathcal{K}^{(3)} \in \mathbb{R}^{3 \times 3 \times 64 \times 64}$ and $\mathcal{K}^{(4)} \in \mathbb{R}^{3 \times 3 \times 64 \times 128}$.

We also do not compress the first CONV layer of O-Net due to the same reason as in SimpNet. Table III shows the overall model compression result employing HOTCAKE. We achieved at least 3× compression ratio on all the three CONV layers even though the original layer sizes are already small enough. Table IV further illustrates the detailed performance of the compressed model. The face classification accuracy decreases less than 1% compared with the original model, at the same time the loss increment of the three tasks are all negligible.

C. Experiments on AlexNet

The third model we use is AlexNet [1] which is much larger than the above two examples. It contains 61.1M parameters in total. Again, we compressed all its CONV layers except the

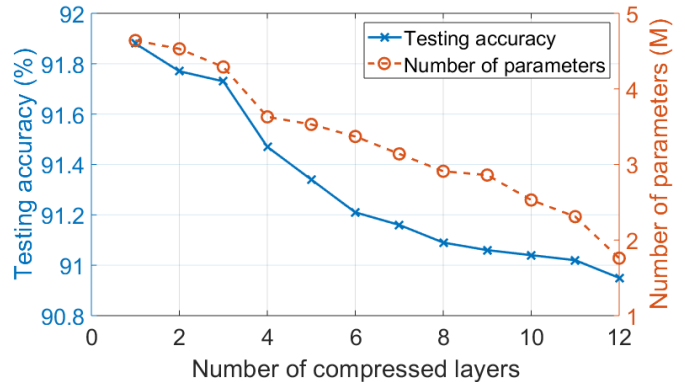


Fig. 4. Classification accuracy and model parameters vs. the number of compressed CONV layers. We compressed the layers in an order w.r.t. the compression ratios. For example, if only 1 layer is compressed, we choose the 5th CONV layer since it has the highest compression ratio. If 2 layers are compressed, the 5th and 12th layers are chosen, and so on. The solid curve shows how accuracy decreases when more layers are compressed. The dotted curve shows how number of parameters changes.

TABLE III
O-NET’S LAYER-WISE ANALYSIS. NUMBERS IN BRACKETS ARE COMPRESSION RATIOS.

No. of compressed CONV layers	Original	HOTCAKE
2	18K	4K (4.50×
3	37K	8K (4.63×
4	33K	11K (3.00×

first. Table V shows the layer-wise analysis of AlexNet. We observe that HOTCAKE can achieve higher compression ratio for each layer. Table VI further shows classification performance of the compressed models. Tucker-2 obtains a higher accuracy when its compression ratio is half less than HOTCAKE. To make the comparison fair, we further set ranks manually for Tucker-2 to reach the same compression ratio as HOTCAKE, and its classification accuracy drops from 90.29% to 81.39%, which is lower than that of HOTCAKE (83.17%). Next, we assign ranks for both Tucker-2 and HOTCAKE, to reach higher compression ratios at around 12×, 14×, and 16×. The results are illustrated in Fig. 5 wherein it is seen that HOTCAKE achieves a higher classification accuracy than Tucker-2 on all the three compression ratios, which indicates the superiority of HOTCAKE over Tucker-2 in high compression ratios.

TABLE VI
AN OVERVIEW OF ALEXNET’S PERFORMANCE AND NUMBER OF PARAMETERS BEFORE AND AFTER COMPRESSION.

	Original	Tucker-2	HOTCAKE
Testing Accuracy	90.86%	90.29%	83.17%
Overall Parameters (CONV layers)	2.47M	520K	261K
Compression Ratio		4.75×	9.37×

TABLE IV
PERFORMANCES OF MTCNN BEFORE AND AFTER COMPRESSION.

	Original	HOTCAKE
Face Classification Accuracy	95.36%	94.42%
Loss of Face Detection	0.648	0.686
Loss of Bounding Box	0.0137	0.0175
Loss of Face Landmarks	0.0107	0.0128
Total loss	0.546	0.569

TABLE V
ALEXNET’S LAYER-WISE ANALYSIS. NUMBERS IN BRACKETS ARE COMPRESSION RATIOS COMPARED WITH THE ORIGINAL CONV LAYERS.

No. of compressed CONV layer	Original	Tucker-2	HOTCAKE
2	307K	127K (2.42 \times)	56K (5.48 \times)
3	664K	197K (3.37 \times)	120K (5.53 \times)
4	885K	124K (7.14 \times)	51K (17.35 \times)
5	590K	71K (8.31 \times)	34K (17.35 \times)

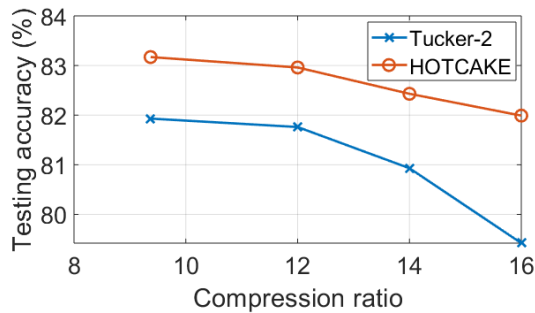


Fig. 5. Accuracy vs. compression ratio on CIFAR-10.

V. CONCLUSION

This paper has proposed a general procedure named HOTCAKE for compressing convolutional layers in neural networks. We demonstrate through experiments that HOTCAKE can not only compress bulky CNNs trained through conventional training procedures, but it is also able to exploit redundancies in various compact and portable network models. Compared with Tucker-2 decomposition, HOTCAKE reaches higher compression ratios with a graceful decrease of accuracy. Furthermore, HOTCAKE can be selectively used for specific layers to achieve targeted and deeper compression, and provide a systematic way to explore better trade-offs between accuracy and the number of parameters. Importantly, this proposed approach is powerful yet flexible to be jointly employed together with pruning and quantization.

REFERENCES

- [1] A. Krizhevsky, I. Sutskever, and G. E. Hinton, “Imagenet classification with deep convolutional neural networks,” in *Advances in neural information processing systems*, 2012, pp. 1097–1105.
- [2] D. Silver, A. Huang, C. J. Maddison, A. Guez, L. Sifre, G. Van Den Driessche, J. Schrittwieser, I. Antonoglou, V. Panneershelvam, M. Lanctot *et al.*, “Mastering the game of go with deep neural networks and tree search,” *nature*, vol. 529, no. 7587, p. 484, 2016.

- [3] G. E. Hinton, N. Srivastava, A. Krizhevsky, I. Sutskever, and R. R. Salakhutdinov, “Improving neural networks by preventing co-adaptation of feature detectors,” *arXiv preprint arXiv:1207.0580*, 2012.
- [4] S. Han, J. Pool, J. Tran, and W. Dally, “Learning both weights and connections for efficient neural network,” in *Advances in neural information processing systems*, 2015, pp. 1135–1143.
- [5] Y. He, X. Zhang, and J. Sun, “Channel pruning for accelerating very deep neural networks,” in *Proceedings of the IEEE International Conference on Computer Vision*, 2017, pp. 1389–1397.
- [6] H. Li, A. Kadav, I. Durdanovic, H. Samet, and H. P. Graf, “Pruning filters for efficient convnets,” *arXiv preprint arXiv:1608.08710*, 2016.
- [7] F. Li, B. Zhang, and B. Liu, “Ternary weight networks,” *arXiv preprint arXiv:1605.04711*, 2016.
- [8] M. Courbariaux, I. Hubara, D. Soudry, R. El-Yaniv, and Y. Bengio, “Binarized neural networks: Training deep neural networks with weights and activations constrained to+ 1 or-1,” *arXiv preprint arXiv:1602.02830*, 2016.
- [9] M. Rastegari, V. Ordonez, J. Redmon, and A. Farhadi, “Xnor-net: Imagenet classification using binary convolutional neural networks,” in *European Conference on Computer Vision*. Springer, 2016, pp. 525–542.
- [10] E. L. Denton, W. Zaremba, J. Bruna, Y. LeCun, and R. Fergus, “Exploiting linear structure within convolutional networks for efficient evaluation,” in *Advances in neural information processing systems*, 2014, pp. 1269–1277.
- [11] V. Lebedev, Y. Ganin, M. Rakhuba, I. Oseledets, and V. Lempitsky, “Speeding-up convolutional neural networks using fine-tuned CP-decomposition,” *arXiv preprint arXiv:1412.6553*, 2014.
- [12] Y.-D. Kim, E. Park, S. Yoo, T. Choi, L. Yang, and D. Shin, “Compression of deep convolutional neural networks for fast and low power mobile applications,” *CoRR*, vol. abs/1511.06530, 2016.
- [13] K. Hayashi, T. Yamaguchi, Y. Sugawara, and S.-i. Maeda, “Einconv: Exploring unexplored tensor decompositions for convolutional neural networks,” *arXiv preprint arXiv:1908.04471*, 2019.
- [14] E. Shelhamer, J. Long, and T. Darrell, “Fully convolutional networks for semantic segmentation,” *IEEE Transactions on Pattern Analysis & Machine Intelligence*, no. 4, pp. 640–651, 2017.
- [15] T. G. Kolda and B. W. Bader, “Tensor decompositions and applications,” *SIAM Review*, vol. 51, no. 3, pp. 455–500, 2009.
- [16] A. Cichocki, D. Mandic, L. D. Lathauwer, G. Zhou, Q. Zhao, C. Caiafa, and A.-H. Phan, “Tensor decompositions for signal processing applications: From two-way to multiway component analysis,” *IEEE Signal Processing Magazine*, vol. 32, no. 2, pp. 145–163, 2015.
- [17] N. Halko, P.-G. Martinsson, and J. A. Tropp, “Finding structure with randomness: Probabilistic algorithms for constructing approximate matrix decompositions,” *SIAM review*, vol. 53, no. 2, pp. 217–288, 2011.
- [18] L. De Lathauwer, B. De Moor, and J. Vandewalle, “A multilinear singular value decomposition,” *SIAM journal on Matrix Analysis and Applications*, vol. 21, no. 4, pp. 1253–1278, 2000.
- [19] —, “On the best rank-1 and rank-(r_1, r_2, \dots, r_m) approximation of higher-order tensors,” *SIAM journal on Matrix Analysis and Applications*, vol. 21, no. 4, pp. 1324–1342, 2000.
- [20] S. H. Hasanpour, M. Rouhani, M. Fayyaz, M. Sabokrou, and E. Adeli, “Towards principled design of deep convolutional networks: introducing simpnet,” *arXiv preprint arXiv:1802.06205*, 2018.
- [21] K. Zhang, Z. Zhang, Z. Li, and Y. Qiao, “Joint face detection and alignment using multitask cascaded convolutional networks,” *IEEE Signal Processing Letters*, vol. 23, no. 10, pp. 1499–1503, Oct 2016.
- [22] A. Krizhevsky, G. Hinton *et al.*, “Learning multiple layers of features from tiny images,” Citeseer, Tech. Rep., 2009.